Proceedings of ASME Turbo Expo 2011
GT2011
June 6-10, 2011, Vancouver, British Columbia, Canada

GT2011-45988

DESIGN OF A HIGHLY LOADED TRANSONIC TWO-STAGE FAN USING SWEPT AND BOWED BLADING

Hailiang Jin
Aeroengine Numerical Simulation Research Center, School of Jet Propulsion, Beijing University of Aeronautics and Astronautics
Beijing, China

Donghai Jin
Aeroengine Numerical Simulation Research Center, School of Jet Propulsion, Beijing University of Aeronautics and Astronautics
Beijing, China

Fang Zhu
Aeroengine Numerical Simulation Research Center, School of Jet Propulsion, Beijing University of Aeronautics and Astronautics
Beijing, China

Ke Wan
Aeroengine Numerical Simulation Research Center, School of Jet Propulsion, Beijing University of Aeronautics and Astronautics
Beijing, China

Xingmin Gui
Aeroengine Numerical Simulation Research Center, School of Jet Propulsion, Beijing University of Aeronautics and Astronautics
Beijing, China

ABSTRACT

This paper presents the design of a highly loaded transonic two-stage fan using several advanced three-dimensional blading techniques including forward sweep and “hub bending” in rotors and several bowed configurations in stators. The effects of these blading techniques on the performance of the highly loaded transonic two-stage fan were investigated on the basis of three-dimensional Navier-Stokes predictions. The results indicate that forward sweep has insignificant impact on the total pressure ratio and adiabatic efficiency of the fan. The throttling range of the fan is found to be improved by forward sweep because the shock in the forward swept rotor is expelled later upstream to the leading edge than that in the unswept one. Hub bending design technique increases the efficiency in the hub region of R1 due to the reduction of the low momentum zone in the hub region near the trailing edge. The stator vane design has a pronounced impact on the performance of the fan. The total pressure ratio, adiabatic efficiency, and stall margin of the schemes with the bowed vanes are increased significantly compared to the scheme with the straight vanes. The large corner stall in the straight S1 vane is reduced effectively by the bowed S1 vanes. Moreover, the strong corner stall in the straight S2 vane is fully eliminated by the bowed S2 vanes. Among the bowed vane schemes, the scheme with positive bowed (P. B.) hub and negative bowed (N. B.) tip vanes has the best efficiency and stall margin performances thanks to the superiority of the performance over the midspan regions of the bowed vanes.

INTRODUCTION

The development of high thrust/weight aircraft gas turbine engines requires compression systems with high pressure ratio, high efficiency, and sufficient stall margin. Using high tip speed is an effective approach to increase the stage pressure ratio of the fan. However, the resulting high Mach number will increase the shock losses and reduce the efficiency and stall margin. Studies suggest that swept design can help to improve high speed fan performance by overcoming these losses. Swept design was firstly applied to the NASA-Lewis QF-12 quiet high speed fan to reduce the fan noise between 1974 and 1977 [1, 2]. Wennerstrom firstly introduced swept design into the highly loaded transonic fan in the famous HTFC program [3, 4]. Wright laboratory designed and tested a series of test rotors to investigate the effects of swept blade [5, 6]. The test results of General Electric and Allison forward swept fan have demonstrated the potential of significant improvements in both efficiency and stall margin with forward swept blading [7]. Experimental and analytical studies conducted by Wadia et al. [8, 9] demonstrated the significant improvements in stall margin and efficiency associated with forward sweep. Denton and Xu [10] investigated the genuine effects of sweep or lean on the flow and the performance of the fan and demonstrated the significant influence on the stall margin using numerical method. Gallimore et al. [11] showed that sweep was effective at reducing the cross passage flow near the hub and interaction between the hub endwall and profile boundary layers in axial compressor rotors. In recent years, Beijing University of Aeronautics and Astronautics (BUAA) successfully designed and tested two highly loaded transonic backward swept single-stage fans ATS-2 [12] and J285 [13] with design pressure ratios of 2.2 and 2.3, respectively. On the other hand, large turning stator vanes are frequently encountered in highly loaded transonic fans, and the most typical flow feature in these stator vanes is corner stall which has great influence on the overall losses of the fan. Wind tunnel experiments conducted by Breugelmans [14] and Shang [15] showed that corner stall could be reduced by leaned and bowed vanes. Weingold et al. [16] demonstrated that the bowed vanes could increase the pressure ratio and efficiency of a three-stage high-speed compressor from the choke limit through surge conditions. Gummer et al. [17] investigated the sweep and dihedral effects in transonic stators of axial compressors numerically and experimentally and demonstrated that positive sweep and positive dihedral could reduce endwall losses and increase the operating range on compressor stators. Fischer et al. [18] investigated the performance of strongly bowed stators in a four-stage high speed compressor and demonstrated the increase in static pressure ratio, total pressure ratio, and overall efficiency of the compressor by the bowed vanes. The effects of swept stator vanes in a highly loaded transonic two-stage fan were investigated with numerical analysis and showed that the corner stall in the hub region was reduced effectively by the swept vanes [19].

This paper presents the design of a highly loaded transonic two-stage fan for a high thrust/weight aircraft gas turbine engine. In order to improve the performance of the two-stage fan, several advanced three-dimensional blading techniques including forward sweep and hub bending in rotors and several bowed configurations in stators were adopted in the fan design. The effects of these blading techniques on the performance of the two-stage fan were investigated on the basis of three-dimensional Navier-Stokes predictions. It is expected that the results could provide the designers with some helpful references in the aerodynamic design of the similar fans.

DESIGN OF THE TWO-STAGE FAN

Pressure ratios and efficiencies are distributed carefully between the first and second stages according to the design targets of the two-stage fan. The flow coefficients and work coefficients of the two stages must be evaluated during the loading distribution procedure to meet certain criteria. A high tip speed is used due to the high design pressure ratio of the fan. However, the resulting high Mach numbers will increase the shock loss and reduce the efficiency of the fan. The precompression profile is utilized in the tip region of the first rotor to reduce the inlet relative Mach number. The specific flow at the inlet of the fan is also an important design parameter which is directly related to the inlet axial Mach number. The inlet axial Mach number of the fan seldom exceeds 0.7 which is limited by the danger of choking in the intake. In this paper, the specific flow at the inlet of the first rotor is 206.8 $kg/s{\cdot}m^2$ and the corresponding inlet axial Mach number is 0.62. Compromise has to be made between aerodynamic performance and mechanical structure in the selection of the inlet hub/tip ratio of the fan. A lower hub/tip ratio (resulting in lower specific flow) is beneficial to aerodynamic performance, but not of structure strength. The hub/tip ratio used in modern transonic fan is lower, about 0.3. In this work, the hub/tip ratio at the inlet of the first rotor is 0.299, slightly lower than the typical value. The contracted casing of the first rotor can help to reduce the inlet relative Mach number and increase the axial velocity ratio in the tip region of the first rotor. The two-stage fan is designed using the streamline curvature throughflow method and arbitrary camber lines blading method [20, 21]. Considering the high loading in the hub region and the clearance leakage flow effect in the tip region, the work is distributed lower in the hub and tip regions than in the midspan region of the first rotor. The work distribution of the second rotor is nearly uniform throughout the whole span due to the high hub/tip ratio of the second rotor. The flow through the first stator does not turn to the axial direction which can reduce the first stator loading and provide certain levels of inlet prewhirl for the second rotor. During the design procedure of the two-stage fan, some design criteria including diffusion factor at rotor tip, axial velocity ratio at rotor tip, diffusion factor at stator hub and inlet absolute Mach number at stator hub must be satisfied. Three-dimensional Navier-Stokes computation is employed to obtain the aerodynamic performance of the fan. Modifications are then made to the parameters of the throughflow calculation and blading design, and iterations continue until the performance of the fan satisfies the design targets. Table 1 shows some key design parameters of the highly loaded transonic two-stage fan. The details of the design targets are not shown here for confidentiality.

Table 1 Design parameters of the two-stage fan

Design parameters	Values
Corrected first rotor tip speed /(m/s)	502.34
Specific flow at the inlet of the first rotor /($kg/s{\cdot}m^2$)	206.80
Tip flow coefficient of the first stage	0.4042
Tip flow coefficient of the second stage	0.3773
Tip work coefficient of the first stage	0.3313
Tip work coefficient of the second stage	0.3599
Relative Mach number at the inlet of the first rotor tip	1.60
Relative Mach number at the inlet of the second rotor tip	1.21
Hub/tip ratio at the inlet of the first rotor	0.299
Hub/tip ratio at the inlet of the second rotor	0.650

Figure 1 shows the flow path of the two-stage fan for the design schemes with forward swept rotors (see table 2). The flow path of the design scheme with unswept rotors has the identical hub and shroud contours except the meridional projection of the leading and trailing edges in the tip regions of R1 and R2, which is not shown here.

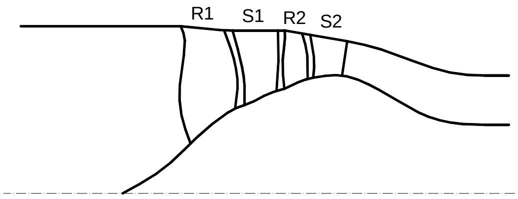

Fig.1 Flow path of the two-stage fan

To improve the performance of the highly loaded transonic two-stage fan, several advanced three-dimensional blading techniques are utilized which yield 6 design schemes of the two-stage fan (see table 2).

For the rotors, the blading techniques are as follows:

a. Unswept,
b. Forward swept tip,
c. Hub bending.

For the stators, the following techniques are adopted:

d. Straight vane,
e. Positive bowed hub,
f. Positive bowed hub and tip,
g. Positive bowed hub and negative bowed tip.

Some descriptions about the “hub bending” design technique are presented here. It is somewhat like the “end bending” and implemented by reducing the aerodynamic loading sharply within small spanwise ranges in the hub region. In this paper, the hub bending design in R1 is implemented through the rapid deviation angle decrease in the hub region. Table 2 summarizes the blading features for different design schemes of the two-stage fan.

Table2 Blading features for different design schemes

Design schemes	R1	S1	R2	S2
Unswept	a + c	e	a	e
Conventional R1	b	e	b	e
Forward swept, (Hub bending R1) , (P. B. hub)	b + c	e	b	e
Straight	b + c	d	b	d
P. B. hub and tip	b + c	f	b	f
P. B. hub and N. B. tip	b + c	g	b	g

THREE-DIMENSIONAL NAVIER-STOKES COMPUTATIONS

The finite-volume based Navier-Stokes solver FINE Turbo by NUMECA International [22] was used to investigate the effects of swept and bowed blading on the performance of the two-stage fan. Rotor tip clearances were considered in the three-dimensional computations. R1 tip clearance is 0.8 mm, about 0.35% of the span. R2 tip clearance is 0.6 mm, about 0.4% of the span. The two-stage fan is meshed with 1227387 grid points, including 17 radial grid points for the rotor tip clearance. The spacing of the first layer grid point at the solid surfaces is $5*10^{-6}$ meters. Figure 2 shows the computational grid of the forward swept scheme. The Spalart-Allmaras turbulence model is adopted for its excellent behavior of prediction precision and numerical stability. Total pressure, total temperature and the direction of the flow are imposed at the inlet of the computational domain. Static pressure is imposed at the outlet and ruled by the simple radial equilibrium. Adiabatic nonslipping condition is applied at the solid boundaries.

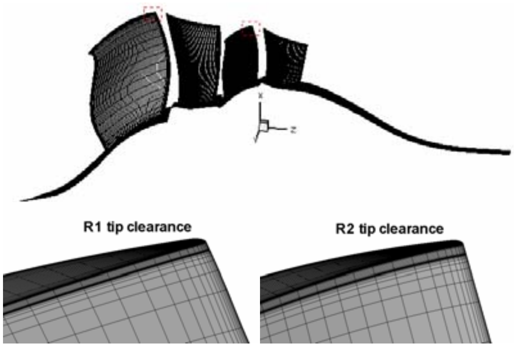

Fig. 2 Computational grid of the two-stage fan

RESULTS AND DISCUSSION

Effects of forward swept rotors on the performance of a highly loaded transonic two-stage fan

Forward sweep design technique is used at the tips of the rotors. In this work, forward sweep is introduced by restacking the tip sections of the unswept rotors along the chord line in a manner similar to that described by Denton and Xu [10]. The chord lengths at the tips of the forward swept rotors are remained as the unswept ones. Hence the pure forward sweep effects on the flowfields of the fan are considered in the rotor design. Figure 3 and Fig. 4 show the comparisons of the unswept and forward swept blading results of R1 and R2.

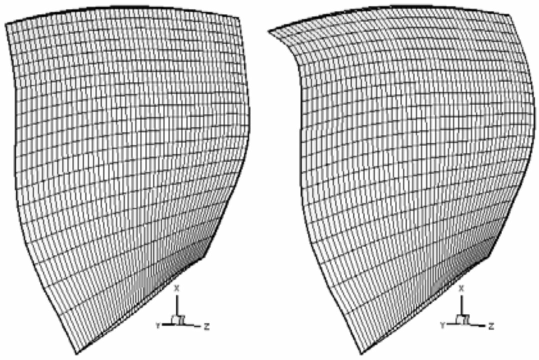

(a) Unswept (b) Forward swept
Fig. 3 Blading results of R1

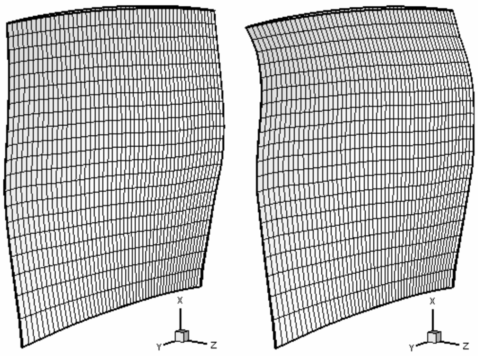

(a) Unswept (b) Forward swept

Fig. 4 Blading results of R2

Figure 5 and Fig. 6 show the comparisons of the performance characteristics (normalized with the design values) between the unswept and forward swept schemes. Figure 5 shows that the choked mass flow of the unswept scheme is slightly higher than its forward swept counterpart. The forward swept scheme can be throttled to a lower mass flow than the unswept scheme as shown in Fig. 5. Hence the forward sweeps in the rotors improve the stall margin of the forward swept scheme. A slight improvement in adiabatic efficiency is provided by the forward swept rotors compared to the unswept scheme. The effects of forward swept rotors on the efficiency of the fan are insignificant.

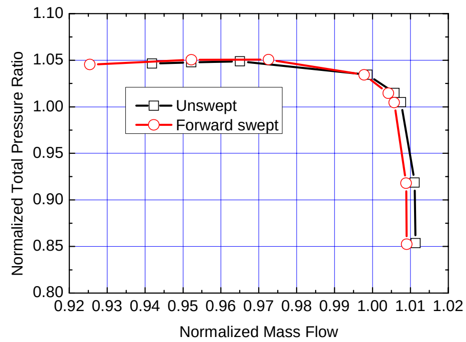

Fig. 5 Performance characteristic of total pressure ratio

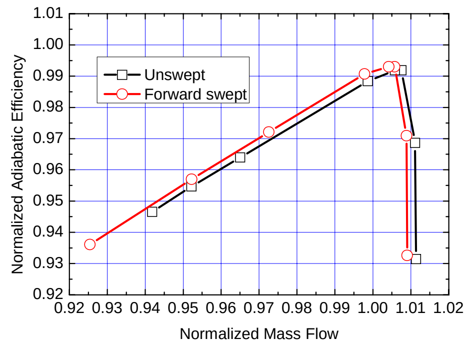

Fig. 6 Performance characteristic of adiabatic efficiency

In order to assess the effects of forward sweep on the performance of the fan, radial distributions of total pressure ratio and adiabatic efficiency (normalized with their design values) of R1 and R2 at near design point are shown in Figs. 7 through 10. Figure 7 shows that the loading of R1 is reduced by forward sweep especially in the tip region which can be demonstrated by the total pressure ratio decrease. The total pressure ratio of the forward swept R2 is slightly higher than the unswept one in the midspan region. The total pressure ratio of R2 must increase to compensate the total pressure ratio decrease of R1 due to the same static pressure distributions at the outlets of the unswept and forward swept schemes. The unswept and forward swept R1 and R2 have nearly the same efficiency distributions as shown in Fig. 9 and Fig. 10. Hence the effects of forward sweep on the efficiency of rotors are insignificant.

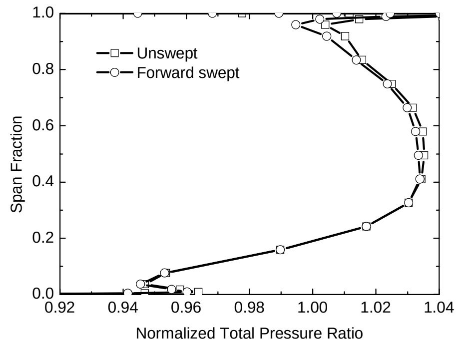

Fig. 7 Radial distributions of the total pressure ratio of R1

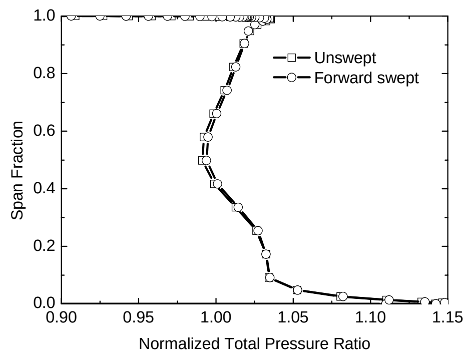

Fig. 8 Radial distributions of the total pressure ratio of R2

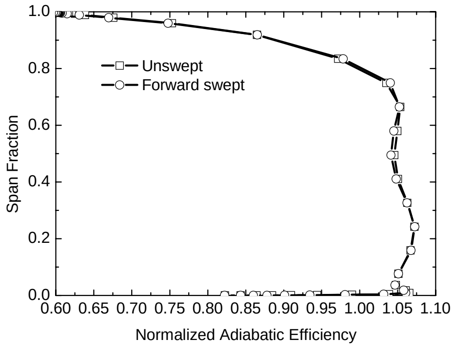

Fig. 9 Radial distributions of the adiabatic efficiency of R1

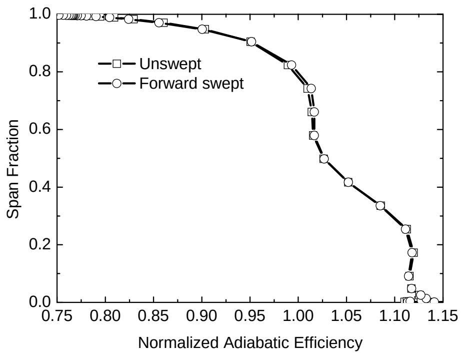

Fig. 10 Radial distributions of the adiabatic efficiency of R2

Figure 11 shows the static pressure distributions (normalized with the total pressure at the fan inlet) on blade surfaces at 95% span of the unswept and forward swept R1 and R2 at near design point. Figure 11 shows that the shock positions are further downstream on the profiles of the forward swept R1 and R2 compared to the unswept ones. The shock position which is further downstream in the tip region, leads to a better stall margin because the rotor can be throttled further until the bow shock detaches from the leading edge.

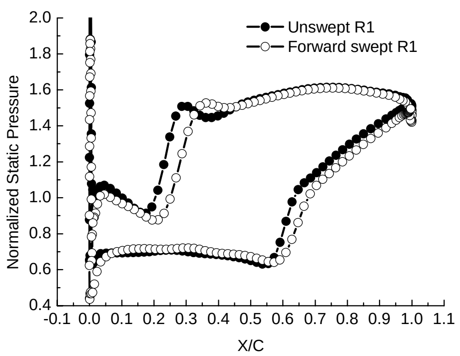

(a) R1

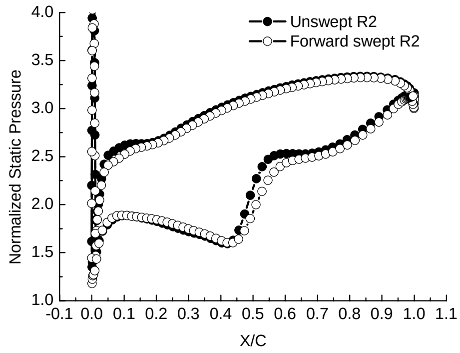

(b) R2

Fig. 11 Static pressure distributions on blade surfaces at 95% span of R1 and R2 at near design condition

Effects of hub bending rotors on the performance of a highly loaded transonic two-stage fan

The hub/tip ratio at the inlet of a modern highly loaded transonic fan is low. As a result of a much lower rotating speed the aerodynamic loading is very high at the rotor hub. Despite the lower reaction there is still a considerable turning at the rotor hub. Due to the high loading flow separation occurs at the rotor hub. Moreover, the large turning also results in a high inlet absolute Mach number at the adjacent downstream stator hub and therefore worsens the stator performance. These disadvantages can be improved by using the "hub bending" technique which is somewhat like the "end bending". The hub bending technique is only applied to R1 in this work. Figure 12 shows the sharp deviation angle decrease in the hub region of the hub bending R1. Figure 13 shows the comparison of conventional (black) and hub bending (red) R1.

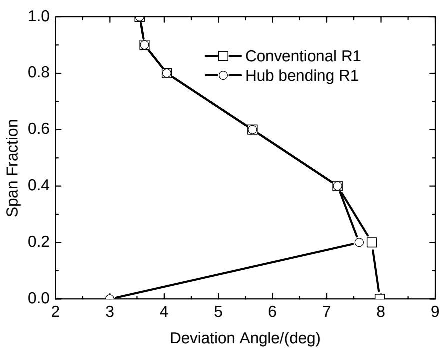

Fig. 12 Deviation angles for conventional and hub bending R1

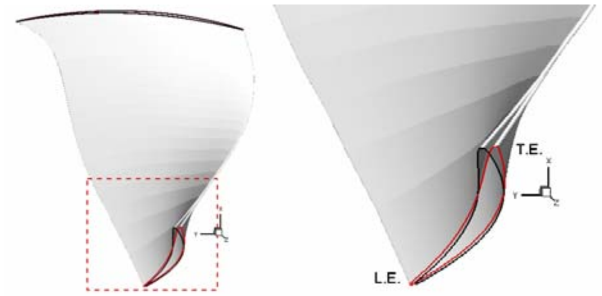

Fig. 13 Comparison of conventional (black) and hub bending (red) R1

Figure 14 and Fig. 15 show the performance characteristics (also normalized with the design values) of the schemes with conventional and hub bending R1 rotors. The scheme with the hub bending R1 has a similar total pressure ratio characteristic but can be throttled to a lower mass flow than its conventional counterpart (see Fig. 14). Hence the scheme with hub bending R1 has a better stall margin. Figure 15 shows that the adiabatic efficiency characteristic of the scheme with the hub bending R1 is very similar to that of the scheme with the conventional R1.

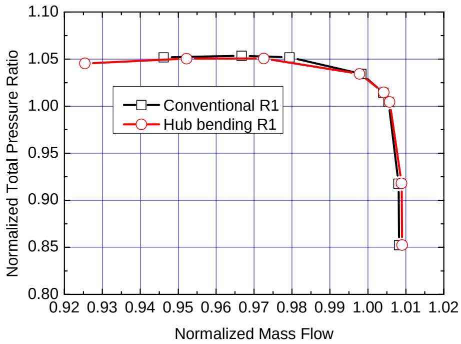

Fig. 14 Performance characteristic of total pressure ratio

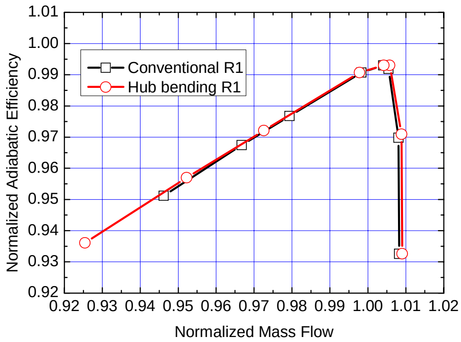

Fig. 15 Performance characteristic of adiabatic efficiency

Radial distributions of total pressure ratio and adiabatic efficiency (normalized with their design values) of R1 at near design point are shown in Fig. 16 and Fig. 17. The spanwise loading of R1 is redistributed by the hub bending design technique. The total pressure ratio of the hub bending R1 is decreased compared to that of the conventional R1 below 40% of the span as shown in Fig. 16. This is because less work is added to the hub region of the hub bending R1. The total pressure ratio above 40% of the span must be increased to compensate for the total pressure ratio decrease in the hub region for the same operating condition of the fan (see Fig. 16). As expected, the adiabatic efficiency of the hub bending R1 is higher than that of the conventional R1 below 25% of the span in Fig. 17. However, the loss reduction in the hub region of the hub bending R1 does not lead to an obvious improvement in the overall efficiency characteristic of the fan (see Fig. 15).

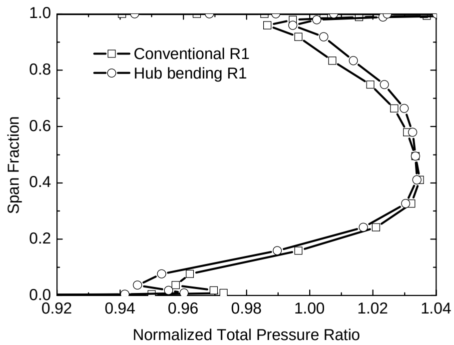

Fig. 16 Radial distributions of the total pressure ratio of R1

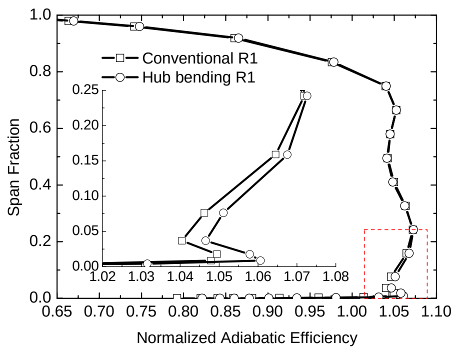

Fig. 17 Radial distributions of the adiabatic efficiency of R1

Figure 18 shows the contours of meridional velocity near the suction surface of conventional and hub bending R1 at near design point. Figure 18 illustrates that the low momentum zone in the hub region near the trailing edge of R1 is reduced by the hub bending design. The resulting loss reduction leads to the adiabatic efficiency improvement in the hub region of the hub bending R1 (see Fig. 17). The reduction of blockage in the hub region of R1 also contributes to the stall margin improvement. In addition, the hub bending design in R1 rotor reduces the inlet absolute Mach number in the hub region of S1 vane indeed which is not shown here.

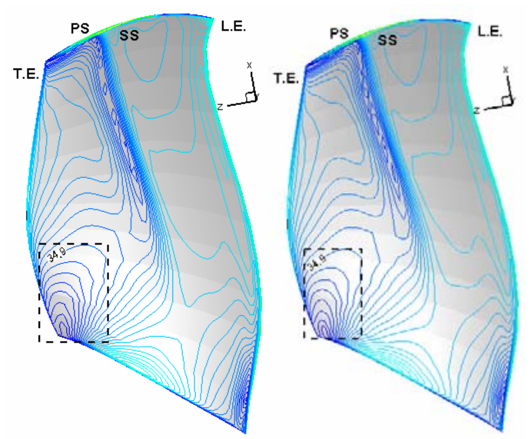

(a) Conventional R1 (b) Hub bending R1

Fig. 18 Contours of meridional velocity near the suction surface of conventional and hub bending R1

Effects of bowed vanes on the performance of a highly loaded transonic two-stage fan

Four different types of stator configurations are used in the stator design: “Straight”, “P. B. hub”, “P. B. hub and tip”, and “P. B. hub and N. B. tip”. The bowed configurations of vanes are introduced by simply restacking the sections of the straight vanes with certain levels of circumferential displacements, which means all these vanes have the same airfoils and vane counts. Figure 19 shows the stacking lines of S1 and S2 vanes (normalized with S1 and S2 spans, respectively). It can be seen from Fig. 19 that the bowed S1 (or S2) vanes have exactly the same hub bowed configurations. The lean angles of the vanes can be easily evaluated from Fig. 19. Table 3 gives the hub and tip lean angles of S1 and S2 vanes. Negative lean angle represents the vane is negative bowed. Figure 20 and Fig. 21 present the blading results of S1 and S2 vanes, respectively.

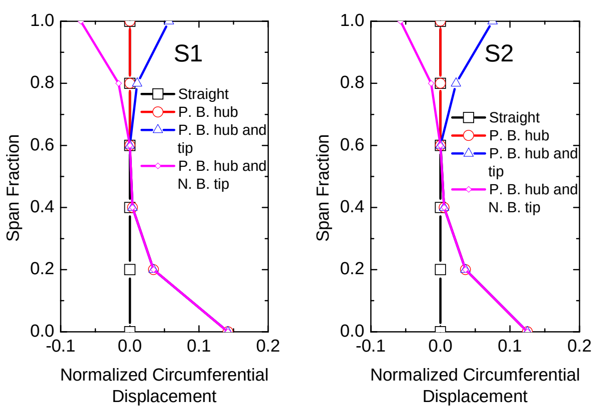

(a) S1 (b) S2

Fig. 19 Stacking lines of S1 and S2 vanes

Table3 Hub and tip lean angles of S1 and S2 vanes

Lean angle/degree	S1 Hub	S1 Tip	S2 Hub	S2 Tip
Straight	0.0	0.0	0.0	0.0
P. B. hub	28.29	0.0	23.99	0.0
P. B. hub and tip	28.29	12.98	23.99	14.71
P. B. hub and N. B. tip	28.29	-15.27	23.99	-12.41

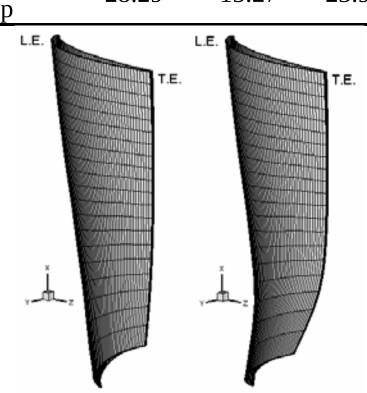

(a) Straight (b) P. B. hub

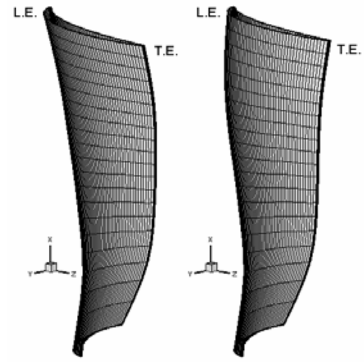

(c) P. B. hub and tip (d) P. B. hub and N. B. tip

Fig. 20 Blading results of S1

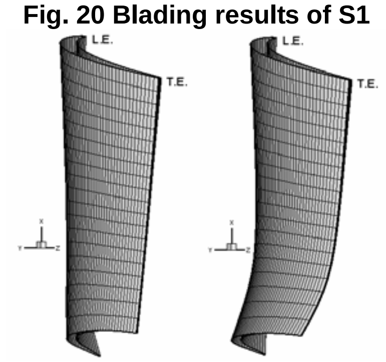

(a) Straight (b) P. B. hub

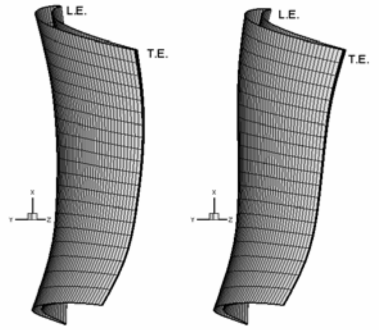

(c) P. B. hub and tip (d) P. B. hub and N. B. tip

Fig. 21 Blading results of S2

Figure 22 and Fig. 23 show the overall performance characteristics (normalized with the design values) of the design schemes with different S1 and S2 vane configurations, respectively. Compared to the straight vane scheme, the total pressure ratio and adiabatic efficiency characteristics are improved significantly in the bowed vane schemes. Figure 22 illustrates that the throttling capabilities (or ranges) of the bowed vane schemes are increased considerably compared to the straight vane counterpart. Figure 23 shows that the adiabatic efficiencies of the bowed vane schemes are increased by about 1.8 points compared with the straight vane scheme at near design point. Among the bowed vane schemes, the total pressure ratio and adiabatic efficiency characteristics are similar. Figure 22 also shows that the P. B. hub and N. B. tip vane scheme has the highest throttling range, followed by the P. B. hub vane scheme, with the P. B. hub and tip vane scheme the lowest.

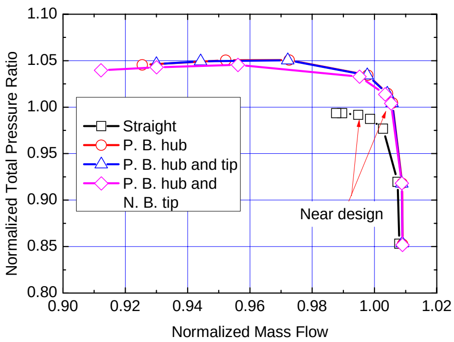

Fig. 22 Performance characteristic of total pressure ratio

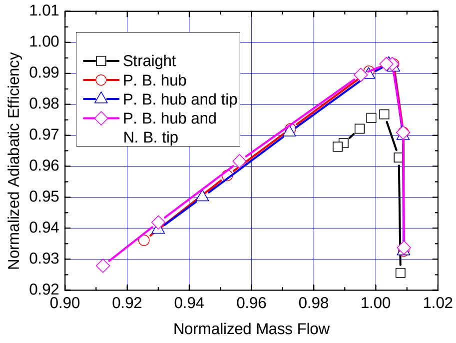

Fig. 23 Performance characteristic of adiabatic efficiency

To identify the contributions of the bowed vanes to the overall performance characteristics of the fan, radial distributions of rotor total pressure ratio, adiabatic efficiency, and stator total pressure recovery coefficient at near design point are shown in Figs. 24 through 29, respectively. All values in Figs. 24 through 29 are normalized with their design values. There is a significant increase of the total pressure ratio of R1 above 30% of the span in the straight vane scheme compared to its bowed vane counterparts in Fig. 24. The total pressure ratio of R2 is increased below 30% of the span but decreased above it in the straight vane scheme. The total pressure ratios of rotors are closely related to the total pressure recovery coefficients of stators. In the straight vane scheme, the higher total pressure ratio of R1 above 30% of the span is mainly attributed to the remarkable decrease of the total pressure recovery coefficient of S1 (see Fig. 28). Since R1 has achieved its maximum loading capacity in the hub region, it must achieve higher total pressure ratios in the midspan and tip regions to compensate the large decrease of the total pressure recovery coefficient of the straight S1 vane for the same design pressure ratio of the fan. The radial distribution of R2 total pressure ratio is affected by both S1 and S2 vanes. Figure 25 shows that the total pressure ratio of R2 is increased in the hub region to compensate the lower total pressure recovery coefficient of the straight S2 vane. On the other hand, the total pressure is lower in the hub region but higher in the tip region at the outlet of the straight S1 vane than that of the bowed S1 vanes. It is another reason for R2 total pressure ratio increase in the hub region but decrease in the tip region. Figure 26 shows that the straight vane scheme has a slightly higher adiabatic efficiency in the tip region of R1 as a result of the higher total pressure ratio. The radial distributions of R1 efficiency are similar in the bowed vane schemes. The higher total pressure ratio in the hub region of R2 leads to a higher adiabatic efficiency in the straight vane scheme (see Fig. 27). The superiority of the bowed vane is demonstrated by the significant increase of total pressure recovery coefficients of the bowed S1 and S2 vanes compared to their straight counterparts in Figs. 28 and 29. It is also noticed that positive bowed tip design increases the total pressure recovery coefficient in the tip region but decreases it in the midspan region among the bowed vanes in Fig. 28 and Fig. 29. Negative bowed tip design is just opposite. By the comprehensive comparison of the effects of the bowed design techniques on the vane performance, it is found that P. B. hub and N. B. tip design is the best, next is P. B. hub design, P. B. hub and tip design is the worst among the bowed vanes.

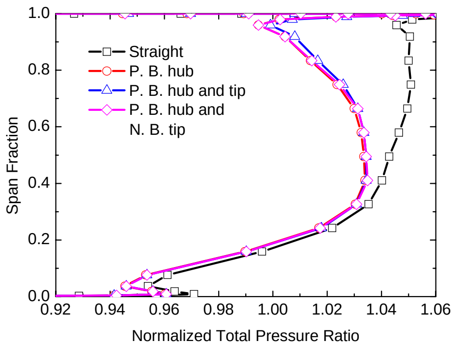

Fig. 24 Radial distributions of the total pressure ratio of R1

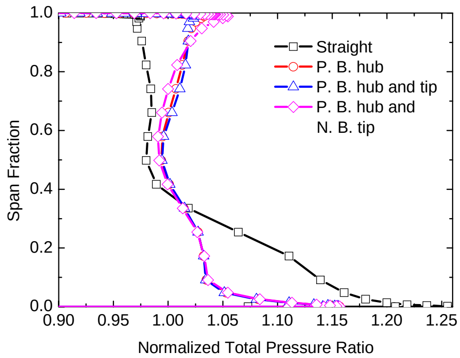

Fig. 25 Radial distributions of the total pressure ratio of R2

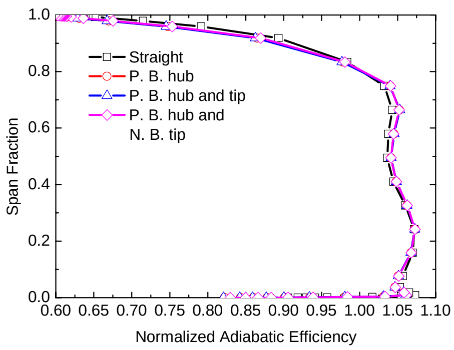

Fig. 26 Radial distributions of the adiabatic efficiency of R1

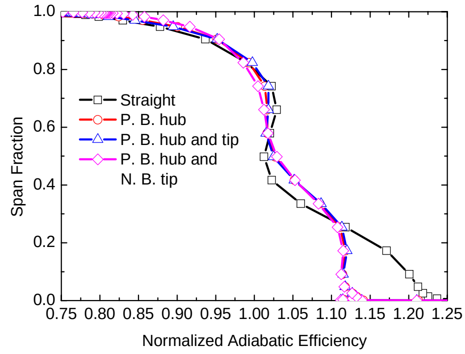

Fig. 27 Radial distributions of the adiabatic efficiency of R2

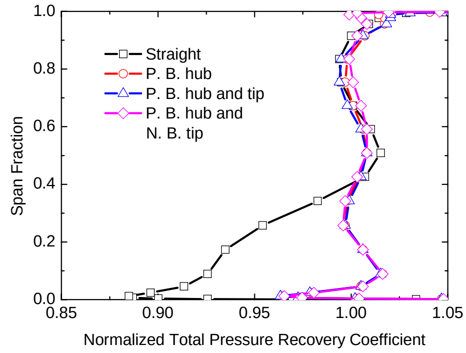

Fig. 28 Radial distributions of total pressure recovery coefficient of S1

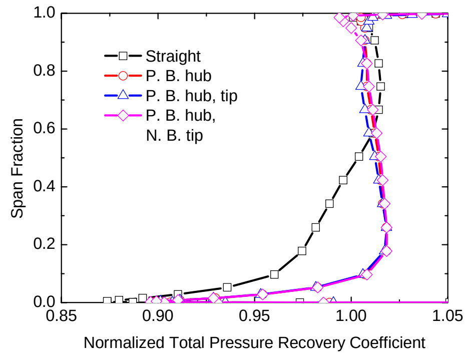

Fig. 29 Radial distributions of total pressure recovery coefficient of S2

To assess the effects of bowed vanes on the performance of the two-stage fan further, Fig. 30 and Fig. 31 show the limiting streamlines on S1 and S2 suction surfaces and hubs at near design condition. A major flow feature of straight and bowed vane configurations is the corner stall flow pattern present at the hub. Corner stall is linked to the presence of at least one three-dimensional separation line, at which the profile and endwall boundary layer interact and separate from the suction surface [17]. When the corner stall grows, a complicated pattern of three-dimensional separation lines, attachment lines, and foci can occur. Reverse flow is probably to be involved in these cases. Figure 30 shows that the large hub corner stall in the straight S1 vane is reduced effectively by its bowed counterparts at near design point. Moreover, the topology of the corner stall in the straight S1 vane changes from foci to three-dimensional separation line in the bowed S1 vanes. Also, the strong hub corner stall in the straight S2 vane passage is fully eliminated by the bowed S2 vanes (see Fig. 31). The elimination of the large hub corner stall reduces the blockage in the straight vane passage. Although limiting streamline distributions of the bowed vanes are similar, some differences still exist. The positive bowed tip design (P. B. hub and tip vane) increases the hub corner stall zone and thus reduces the core flow zone (see Fig. 30 (c) and Fig. 31 (c)). In contrast, the negative bowed tip design (P. B. hub and N. B. tip vane) reduces the hub corner stall zone and extends the core flow zone despite somewhat local flow separation presence in the tip region, and thus improves the performance over the midspan region (see Fig. 30 (d) and Fig. 31 (d)). These flow features are just responsible for the performance behaviors of the stators (see Fig. 28 and Fig. 29). From the above analysis the P. B. hub and N. B. tip vane has the minimal blockage. The blockage in the vane passage will increase the static pressure behind a rotor and the shock is more easily expelled upstream to the leading edge. Hence the blockage reduction in the vane passage can improve the stall margin of the fan. Therefore the P. B. hub and N. B. tip vane scheme attains the largest stall margin thanks to the significant reduction of the blockage in the vanes.

Figure 32 and Fig. 33 show the static pressure (normalized with the total pressure at the fan inlet) in S1 and S2 passage at near design point. Figure 32 and Fig. 33 show that the straight S1 and S2 vanes have the lowest radial gradients of static pressure in the hub regions. Without the limit of the radial gradients of static pressure, flows in the hub regions migrate to the midspan regions resulting in large corner stalls. P. B. hub design technique used in the bowed vanes increases the radial gradient of static pressure in the hub regions. The increasing radial gradients of static pressure constrain the flow migrations to a smaller region, and thus improve the large corner stalls in the hub regions of the straight vanes. On the other hand, N. B. tip design technique decreases the radial gradients of static pressure in the tip region. Also, it helps to suppress the flow migrations from the tip regions to the midspan regions. The features of static pressure in Fig. 32 and Fig. 33 account for the limiting streamlines distribution features in S1 and S2 vanes (see Fig. 30 and Fig. 31).

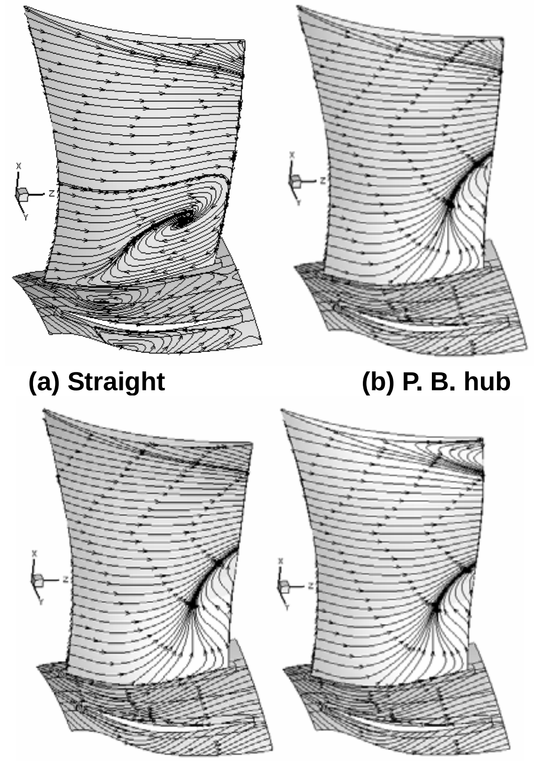

(a) Straight **(b) P. B. hub**

(c) P. B. hub and tip **(d) P. B. hub and N. B. tip**

Fig. 30 Limiting streamlines on the suction surface of S1 and hub at near design condition

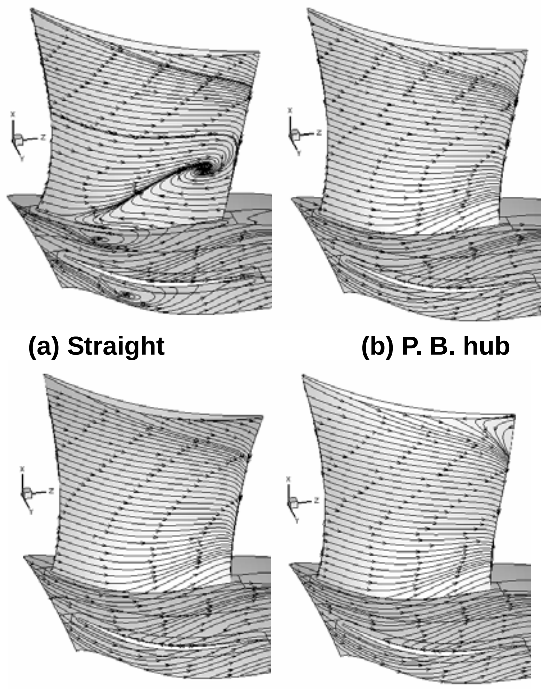

(a) Straight **(b) P. B. hub**

(c) P. B. hub and tip **(d) P. B. hub and N. B. tip**

Fig. 31 Limiting streamlines on the suction surface of S2 and hub at near design condition

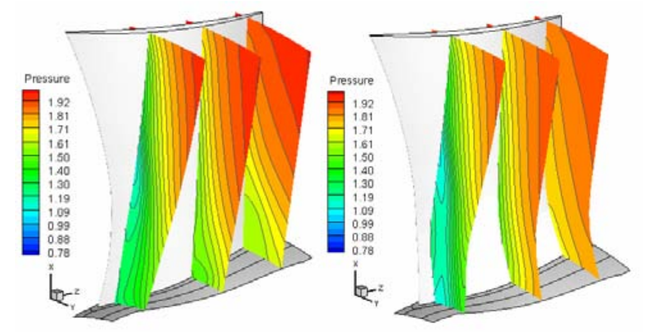

(a) Straight **(b) P. B. hub**

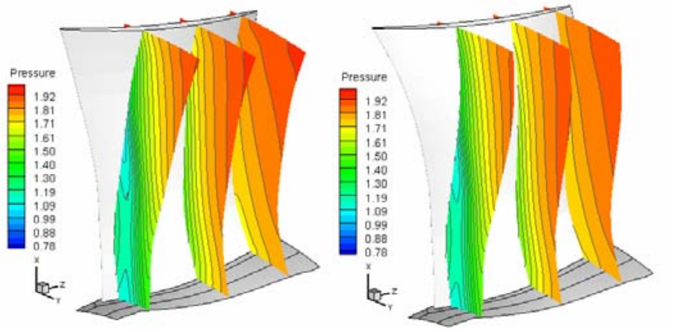

(c) P. B. hub and tip **(d) P. B. hub and N. B. tip**

Fig. 32 Normalized static pressure distribution in S1 passage at near design condition

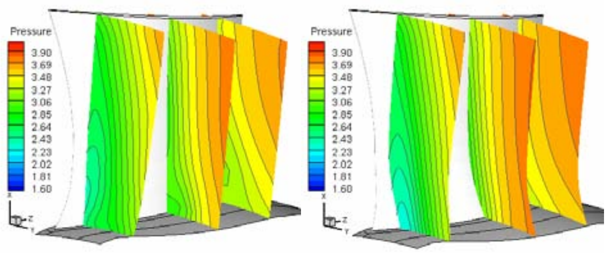

(a) Straight **(b) P. B. hub**

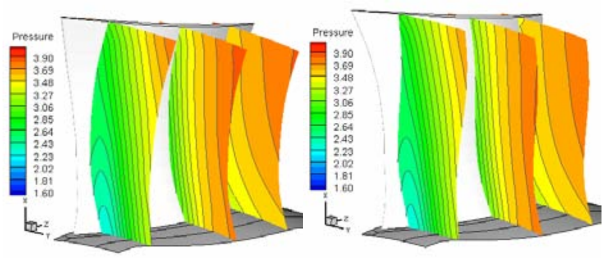

(c) P. B. hub and tip **(d) P. B. hub and N. B. tip**

Fig. 33 Normalized static pressure distribution in S2 passage at near design condition

CONCLUSIONS

Advanced three-dimensional blading techniques including forward sweep and hub bending design techniques in rotors and several bowed configurations in stators, were implemented in a highly loaded transonic two-stage fan and yielded 6 design schemes. The effects of these blading techniques on the performance of the two-stage fan were analyzed on the basis of three-dimensional Navier-Stokes predictions. The results indicate that the effect of forward sweep on the total pressure ratio and adiabatic efficiency of the fan is insignificant. The shock is expelled later upstream to the leading edge with a longer distance in the forward swept rotor than that in the unswept one. This leads to the advantage of stall margin of the forward swept scheme over the unswept one. Hub bending design increases the efficiency in the hub region of R1. The stator vane design has a pronounced impact on the performance of the highly loaded transonic two-stage fan. The total pressure ratio, adiabatic efficiency, and stall margin of the bowed vane schemes are increased significantly compared to the straight vane scheme. The large corner stall involving severe reverse flow in the straight S1 vane is reduced effectively with the topology of corner stall changed from foci to three-dimensional separation line in the bowed S1 vanes. Moreover, the strong corner stall in the straight S2 vane is fully eliminated by the bowed S2 vanes. The reduction of the large blockage in the straight vanes by the bowed vanes improves the stall margin of the two-stage fan significantly. Among these bowed vane schemes, the P. B. hub and N. B. tip vane scheme has the best performances of efficiency and stall margin thanks to the superiority of the performance over the midspan regions of the P. B. hub and N. B. tip vanes.

NOMENCLATURE

L. E.	leading edge
N. B.	negative bowed
P. B.	positive bowed
PS	pressure surface
R1	first stage rotor
R2	second stage rotor
S1	first stage stator
S2	second stage stator
SS	suction surface
T. E.	trailing edge

ACKNOWLEDGMENTS

This work was supported by National Natural Science Foundation of China (50736007，51006005), “Fan-Zhou” Youth Foundation (20100401), and the Fundamental Research Funds for the Central Universities (YWF-10-02-013).

REFERENCES

[1] Bliss, D.B., Hayden, R. P., Murry, B. S., 1976, “Design Considerations for Novel Low Source Noise Transonic Fan Stage”, AIAA-1976-577.

[2] Lucas, R. G., Woodard, R. P., Mackinnon, M. J., 1978, “Acoustic Evaluation of a Novel Swept Rotor Fan”, AIAA-1978-1121.

[3] Wennerstrom, A. J., Frost, G. R., 1976, “Design of a 1500ft/sec, Transonic, High-Through-Flow, Single-Stage Axial-Flow Compressor with Low Hub/Tip Ratio”, AFARL-TR-76-59, AD-B016386.

[4] Wennerstrom, A. J., Derose, R. D., Law, C. W., 1976, “Investigation of a 1500ft/sec, Transonic, High-Through-Flow, Single-Stage Axial-Flow Compressor with Low Hub/Tip Ratio”, AFARL-TR-76-92, AD-B016506.
[5] Frank, B. J., King, P. I., 1994, “Effects of Leading Edge Sweep on Stall Inception in a High-Speed Single-Stage Compressor”, AIAA-1994-2696.
[6] Boger, K.M., King, P. I., Copenhaver, W. W., 1993, “Stall Inception in Single Stage High-Speed Compressor with Straight and Swept Leading Edges”, AIAA-1993-1870.
[7] Kandebo, S. W., 1996, “General Electric Tests Forward Swept Fan Technology”, Aviation Week & Space Technology.
[8] Wadia, A. R., Szucs, P. N. and Crall, D. W., 1997, “Inner Workings of Aerodynamic Sweep”, ASME Paper 1997-GT-401.
[9] Wadia, A. R., Szucs, P. N., Crall, D. W. and Rabe, D. C., 2002, “Forward Swept Rotor Studies in Multistage Fans with Inlet Distortion”, ASME Paper GT-2002-30326.
[10] Denton. J. D. and Xu. L., 2002, “The Effects of Lean and Sweep on Transonic Fan Performance”, ASME Paper GT-2002-30327.
[11] Gallimore, S. J., Bolger, J. J., Cumpsty, N. A., Taylor, M. J., Wright, P. I., Place, J. M. M., 2002, “The Use of Sweep and Dihedral in Multistage Axial Flow Compressor Blading Part I: University Research and Methods Development”, ASME Paper GT-2002-30328.
[12] Peng Shan, Xingmin Gui, 2000, “Final Report for the Design and Experiment Study of a High Loading Single-Stage Model Fan ATS-2 with a Backward Swept Rotor”, Beijing: Beijing University of Aeronautics and Astronautics, GF-A0041935. [in Chinese]
[13] Guorong Hu, Yafeng Zhou, Baoshi Chen et al, 2001, “Design and Test for Single Stage Transonic Fan with High Speed, High Load”, Journal of Engineering Thermophysics, 22(1):40-43. [in Chinese]
[14] Breugelmans, F. A. H. et al., 1984, “Influence of Dihedral on the Secondary Flow in a Two-Dimensional Compressor Cascade”, ASME Journal of Engineering for Gas Turbines and Power, 106, pp. 578–584.
[15] Shang, E. et al., 1993, “The Experimental Investigations on the Compressor Cascades with Leaned and Curved Blade”, ASME, Paper No. 93-GT-50.
[16] Weingold, H. D. et al., 1995, “Reduction of Compressor Stator Endwall Losses Through the Use of Bowed Stators”, ASME, Paper No. 95-GT-380.
[17] Gummer, V., Wenger, U., Kau, H. P., 2001, “Using Sweep and Dihedral to Control Three-Dimensional Flow in Transonic Stators of Axial Compressors”, ASME Journal of Turbomachinery, Vol. 123, pp. 40-48.
[18] Fischer, A., Riess, W., and Joerg, R., Seume, J. R., 2004, “Performance of Strongly Bowed Stators in a Four-Stage High-Speed Compressor”, ASME Journal of Turbomachinery, Vol. 126, pp. 333-338.
[19] Hailiang Jin, Donghai Jin, Xingmin Gui, 2010, “Numerical Investigation of the Effects of Swept Blade on the Aerodynamic Performance of a Highly Loaded Transonic Two-Stage Fan”, The 2010 Asia-Pacific International Symposium on Aerospace Technology (APISAT-2010), Vol. 4, pp.987-992.
[20] Frost, G. R., Wennerstrom, A. J., 1973, “The Design of Axial Compressor Airfoils Using Arbitrary Camber Lines”, ARL-73-0107, AD-765165.
[21] Guofeng Ji, Xingmin Gui, 2009, “A Blading Design Method for Axial/Centrifugal Compressor Airfoils Using Arbitrary Camber Lines”, Journal of Aerospace Power, 24(1):150-156. [in Chinese]
[22] NUMECA Int., 2000, “Numeca’s Flow Integrated Environment for Turbomachinery and Internal Flows”, User Manual, Numeca Int., Brussels, Belgium.

